

Original Article

A Novel Modified Multilevel Inverter for Improved Performance in Renewable Energy Systems

E. Parimalasundar¹, S. Muthukaruppasamy², S. Sendil Kumar³, R. Dharmaprakash⁴, S. Jayakumar⁵, T. Nageswara Prasad⁶

¹Department of Electrical and Electronics Engineering, Mohan Babu University, Tirupati, India.

²Department of Electrical and Electronics Engineering, Velammal Institute of Technology, Panchetti, Tamilnadu, India.

³Department of Electrical and Electronics Engineering, S.A. Engineering College, Chennai, India.

⁴Department of Electrical and Electronics Engineering, Panimalar Engineering College, Chennai, India.

⁵Department of Electronics and Communication Engineering, Sri Sairam College of Engineering, Bengaluru, India.

⁶Department of Electrical and Electronics Engineering, KSRM College of Engineering, Kadapa, India.

¹Corresponding Author : parimalpsg@gmail.com

Received: 08 March 2025

Revised: 13 April 2025

Accepted: 27 April 2025

Published: 31 May 2025

Abstract - Multilevel Inverters (MLIs) are crucial in photovoltaic (PV) systems since they enhance efficiency, reduce Total Harmonic Distortion (THD), and minimize switching losses. There is a comparison between the Cascaded H-Bridge (CHB), the Flying Capacitor (FC), the Neutral Point Clamped (NPC), and a modified MLI design, which is shown in this research. The redesigned inverter, which consists of three DC sources, four diodes, and seven switches, achieves an efficiency of 98%, which is higher than the CHB (96%), FC (95%), and NPC (96%). The performance of the inverter is validated using simulations conducted in MATLAB/Simulink, which include a wide range of modulation indices and load conditions. While the modified topology reduces total power loss to 180W, it produces 308.75V with a THD of 7.3% at $m=0.95$. In contrast, cascaded H-bridges produce 200W and neutral point clamped MLIs produce 220W. A power factor of 0.93 and an efficiency of 93% are achieved by the system when it is subjected to conditions of resistive-inductive load interaction. In comparison to conventional topologies, the MLI that has been proposed reduces switching and conduction losses by around fifteen percent, which guarantees greater voltage balancing and fault tolerance via its implementation. In addition, the inverter functions in a manner that guarantees consistent operation via the use of a simplified control mechanism, which makes it an economical choice for grid-connected solar applications. Based on the findings of the research, it has been established that the redesigned design has increased power quality by a substantial amount, decreased harmonic distortions, and enhanced system reliability, therefore establishing it as a viable alternative for the future generation of renewable energy systems.

Keywords - Efficiency, MATLAB/Simulink, Multilevel Inverter, SPWM, Power Loss, THD.

1. Introduction

The installation of renewable energy sources, particularly Photovoltaic (PV) systems, has been accelerated as a result of the fast depletion of fossil fuels and the growing need for clean energy on a global scale. PV systems have become an essential component of modern power generation due to the fact that they are environmentally friendly, need minimal maintenance, and can be scaled up to meet increasing demand. In order to integrate photovoltaic modules with the utility grid, it is necessary to convert the Direct Current (DC) energy that they generate into Alternating Current (AC) power without any loss of efficiency. Inverters that are characterized by high efficiency, minimum power loss, and decreased Total Harmonic Distortion (THD) are required for the conversion process. This is done to ensure that power quality and grid stability are maintained successfully. As a result of its ability

to generate a stepped AC output waveform, Multilevel Inverters (MLIs) have turned out to be a more desirable alternative to traditional two-level inverters. This is because MLIs are able to THD, switching losses, and voltage stress on semiconductor devices. In applications that need medium- and high-power, such as solar power plants, industrial motors, and smart grids, MLIs are used to a significant degree. Inverters with the Cascaded H-Bridge (CHB), Flying Capacitor (FC), and Neutral Point Clamped (NPC) topologies are the most common types of machine learning inverters. Despite the fact that these topologies provide a number of advantages, they also present challenges, such as significantly increased component counts, complex control systems, and issues in maintaining voltage balance. This research proposes a new MLI topology that reduces the number of switching devices and maximises the efficiency of power conversion. This



topology helps to alleviate the limits that have been imposed. The proposed inverter requires three DC sources, four diodes, and seven switches, which results in a significant reduction in system complexity and expense while simultaneously achieving improved efficiency and fault tolerance. The proposed design achieves reduced switching losses, decreased conduction losses, and enhanced voltage balancing in comparison to conventional MLIs, all without the need for additional capacitors or diodes [1-3].

2. Literature Review

To improve the performance of conventional MLIs, several asymmetric and hybrid topologies have been created to optimise component quantity while preserving or enhancing efficiency. Asymmetric MLIs use varying amplitudes of DC voltage sources, enabling an increased number of voltage levels with a reduced number of switches. Certain designs obviate the need for supplementary H-bridges by directly producing positive, negative, and zero voltage levels, hence reducing switch voltage stress but increasing complexity in control and switching sequences. Although alternative topologies make use of series/parallel configurations of identical DC sources, they reduce the number of switches that are required for maximum performance. However, in order to do this, advanced modulation methods are required. As an additional benefit, H-bridge-based inverters reduce the amount of power that is lost by limiting the number of active switches that are present in the conduction channel. The administration of Total Standing Voltage (TSV), which has an effect on the scalability of high-power systems, is a key challenge in these kinds of environments. For the purpose of preserving voltage homeostasis and avoiding inefficiencies as well as problems with power quality, precise control strategies are very necessary [4-6].

Researchers have focused their efforts on optimizing MLI performance by reducing the number of switching components and using advanced modulation techniques. This is in addition to the advances that have been conducted in topology. Through the reduction of the number of switches, conduction losses can be reduced, system design can be simplified, and reliability can be improved. The Nearest Level Control approach is an effective modulation method that locates the voltage level that is closest to the reference waveform and is thus accessible. This helps to reduce the switching frequency and the power losses that are associated with it significantly.

In comparison to traditional Sinusoidal Pulse Width Modulation (SPWM) and Space Vector Pulse Width Modulation (SVPWM), non-linear control provides a higher degree of efficiency, while also maintaining higher output voltage levels and allowing for smoother operation. Furthermore, with high voltage stress leading to degradation and a shorter lifespan, it is essential to minimize the total static voltage in order to ensure the long-term stability of

components. Modified asymmetric switching approaches have been proposed with the intention of reducing transverse switching voltage, which would ultimately lead to an increase in efficiency and an extension of component lifetime, making them appropriate for grid-connected and renewable energy applications [7-9].

It is possible to demonstrate the benefits of modern MLI topologies via comparative analysis and simulated evaluations. The results of research conducted on asymmetric MLIs with reduced switch counts have shown that these topologies achieve overall harmonic distortion levels that are lower than 5% while maintaining efficiency levels that are higher than 95%. Research reveals that improvements in grounding and insulation techniques have led to breakthroughs in the reduction of leakage and common-mode currents in multilevel inverters that are supplied by solar generation [10]. When it comes to efficiency and the reduction of harmonics, non-linear transformation and Selective Harmonic Elimination (SHE) are superior to traditional modulation approaches. The THD of a proposed 49-level inverter is 1.65%, and its efficiency is 98%. This represents a significant improvement in power quality when compared to conventional CHB, NPC, and FC inverters. The optimization of switch topologies, the reduction of component counts, and the improvement of modulation techniques are the sources of these advancements, which combined result in a reduction of switching losses and TSV [11,12].

Despite great accomplishments, there are still many challenges to overcome. The addition of auxiliary circuits is often required in order to reduce the number of switches involved, which results in an increase in the complexity of the system. In spite of the fact that lowering the number of components is beneficial, it should not lead to a rise in the need for capacitors, an increase in the number of diodes, or more complicated control systems. Scalability for high-power applications is a challenge because of the appearance of growing TSV and voltage imbalance challenges in high-voltage situations. Scalability is a challenge because of these characteristics. Modular Multilevel Converters (MMCs) have an important characteristic in common. Despite the fact that MMCs are widely used in high-power applications, the fact that they need floating capacitors, a large number of switches, and complex control mechanisms makes them less suitable for low- to medium-voltage applications. The inverter that has been recommended provides a viable alternative for grid-connected renewable energy applications and solar systems [13-15].

The integration of Maximum Power Point Tracking (MPPT) with MLIs improves photovoltaic system efficiency but introduces more complexities. Variable environmental circumstances, including fluctuating irradiance and temperature changes, hinder standard MPPT algorithms such as Perturb & Observe (P&O) and Incremental Conductance

(IC) from precisely locating the global maximum power point (GMPP). Accelerated alterations may result in energy losses and inefficiencies. The rapidity of convergence and stability are crucial, since fast tracking enhances power extraction; nevertheless, excessive adjustments may result in voltage instability and oscillations. Advanced MPPT techniques, such as fuzzy logic and artificial intelligence-based methods, improve stability while elevating computing complexity [16-18].

Moreover, MPPT directly impacts the DC link voltage, hence influencing MLI performance. Fluctuations in DC voltage may impair waveform integrity, elevate THD, and interfere with grid synchronisation. Real-time synchronisation between MPPT and MLI control algorithms is essential for steady operation. The use of adaptive DC link voltage regulation, predictive control, and hybrid MPPT techniques guarantees optimum power conversion, reduces switching losses, and enhances overall system dependability. Confronting these obstacles is crucial for attaining high-efficiency, grid-connected photovoltaic systems that can sustain constant power generation amid variable climatic circumstances [19-22].

The following major objectives are considered to make an efficient system of MLI-fed grid system:

- Develop a modified seven-level multilevel inverter that optimizes power quality, minimizes switching losses, and enhances efficiency for renewable energy applications.
- Employ an efficient switching method, such as Sinusoidal Pulse Width Modulation, to reduce Total Harmonic Distortion and enhance waveform quality.
- Minimize conduction and switching losses by using optimized circuit topology and optimal use of power semiconductor devices.
- Assess the inverter's performance over various load circumstances, including Resistive (R) and Resistive-Inductive (RL) loads.
- Perform a comparative study of the modified and conventional MLIs, focusing on characteristics like THD, efficiency, power factor, and modulation index.

3. Modified Seven-Level MLI and its Operating Modes

The modified seven-level multilevel inverter is shown in Figure 1. This inverter is integrated with a solar system and is linked to the utility grid. A solar module, a DC-DC boost converter, a multilevel inverter, a maximum power point tracking controller, and a grid interface are the components that make up the system. Direct current is generated by the photovoltaic module, which transforms solar energy into direct current. This direct current is then controlled by a DC-DC boost converter, which generates a steady DC link voltage conducive to multilevel conversion. Therefore, this ensures that the photovoltaic array is extracted with the maximum

amount of power possible, which in turn improves the system's efficiency and performance. After that, the MLI converts the DC voltage into AC with a lower THD, which ensures a greater power output that is suitable for grid integration applications. When compared to conventional two-level inverters, the MLI presents a considerable reduction in switching losses, conduction losses, and voltage stress on semiconductor components.

As a consequence, the MLI leads to enhanced efficiency and higher system longevity. The typical CHB MLI structure is shown in Figure 2. This structure consists of twelve power switches, which are arranged in a large number of H-bridge cells to generate stepped voltage waveforms. Despite the fact that this design achieves a reduction in harmonic distortion and an improvement in power quality, it requires a greater amount of semiconductor switches, which results in increased switching losses, conduction losses, and control complexity. The substantial quantity of power switches results in diminished overall system efficiency relative to the modified topology, hence requiring a more optimized strategy for multilevel inversion.

Figure 3 illustrates the proposed seven-level MLI, which incorporates three DC sources, four diodes, and just seven switches, therefore substantially minimizing component count, complexity, and expense. The modified MLI significantly decreases switching and conduction losses by about 15%, while ensuring stable voltage balancing and enhanced fault tolerance.

The inverter produces output voltage levels of $\pm 3V_{dc}$, $\pm 2V_{dc}$, $\pm V_{dc}$, and $0V$, facilitating a near-sinusoidal output waveform that reduces THD and enhances overall power conversion efficiency. The proposed system improves dependability and operational simplicity by streamlining the modulation control technique, making it an optimal choice for renewable energy applications, including PV-grid integration and industrial motor drives.

Figure 4 illustrates the $+3V_{dc}$ output voltage level generated by the modified MLI. At this juncture, the inverter functions by activating designated switches (S_1 , S_2 , S_3 , and S_4), enabling the output voltage to reach $+3V_{dc}$. The diodes (D_1 and D_2) are essential for regulating current flow and maintaining voltage equilibrium, so ensuring the inverter output stays steady without imposing undue stress on the power components. The stepped sinusoidal output waveform significantly reduces THD and improves inverter performance, making the topology very energy-efficient and dependable. In Figure 5, the inverter produces $+2V_{dc}$ by activating switches S_1 , S_2 , and S_5 , while the other switches are off. This selective switching technique mitigates conduction losses and decreases the frequency of active switching transitions, hence reducing power dissipation and enhancing the overall efficiency of the inverter.

In comparison to conventional MLIs, the modified MLI guarantees enhanced voltage control and stability, enabling uninterrupted operation under fluctuating load situations. Figure 6 depicts the $+V_{dc}$ output voltage level attained by activating switches S_1 and S_6 . This switching approach guarantees optimized current pathways, hence significantly reducing switching stress on the semiconductor devices. The enhanced current pathway facilitates superior power flow control, reducing power dissipation and augmenting the inverter's performance in renewable energy applications. Figure 7 illustrates an alternate switching configuration for obtaining a $+0V_{dc}$ output voltage. The modified design improves voltage balance and reduces harmonic distortions by modifying the switching sequence. This functionality is essential for enhancing inverter reliability and efficiency, especially in grid-connected systems where voltage control and power quality are important issues. The steps for generating negative voltage are shown in the following images.

Figure 8 illustrates the negative output voltage ($-V_{dc}$) of the inverter, attained by activating switches S_3 and S_7 . This alters the existing trajectory, guaranteeing the inverter's bidirectional power flow capacity, which is crucial for applications such as energy storage systems and bidirectional converters. In Figure 9, the inverter produces $2V_{dc}$ by engaging switches S_3 , S_4 , and S_6 . The switching control method facilitates a seamless transition between voltage levels, reducing voltage stress on power components and enhancing overall efficiency.

Figure 10 illustrates the development of a $-3V_{dc}$ output voltage, achieved when switches S_3 , S_4 , S_5 , and S_7 are activated. The meticulously engineered switching sequence and diode configuration enable seamless and efficient voltage transformation, minimizing THD and power losses. This method guarantees the inverter functions well at elevated modulation indices, making it an ideal option for renewable energy conversion and grid integration applications.

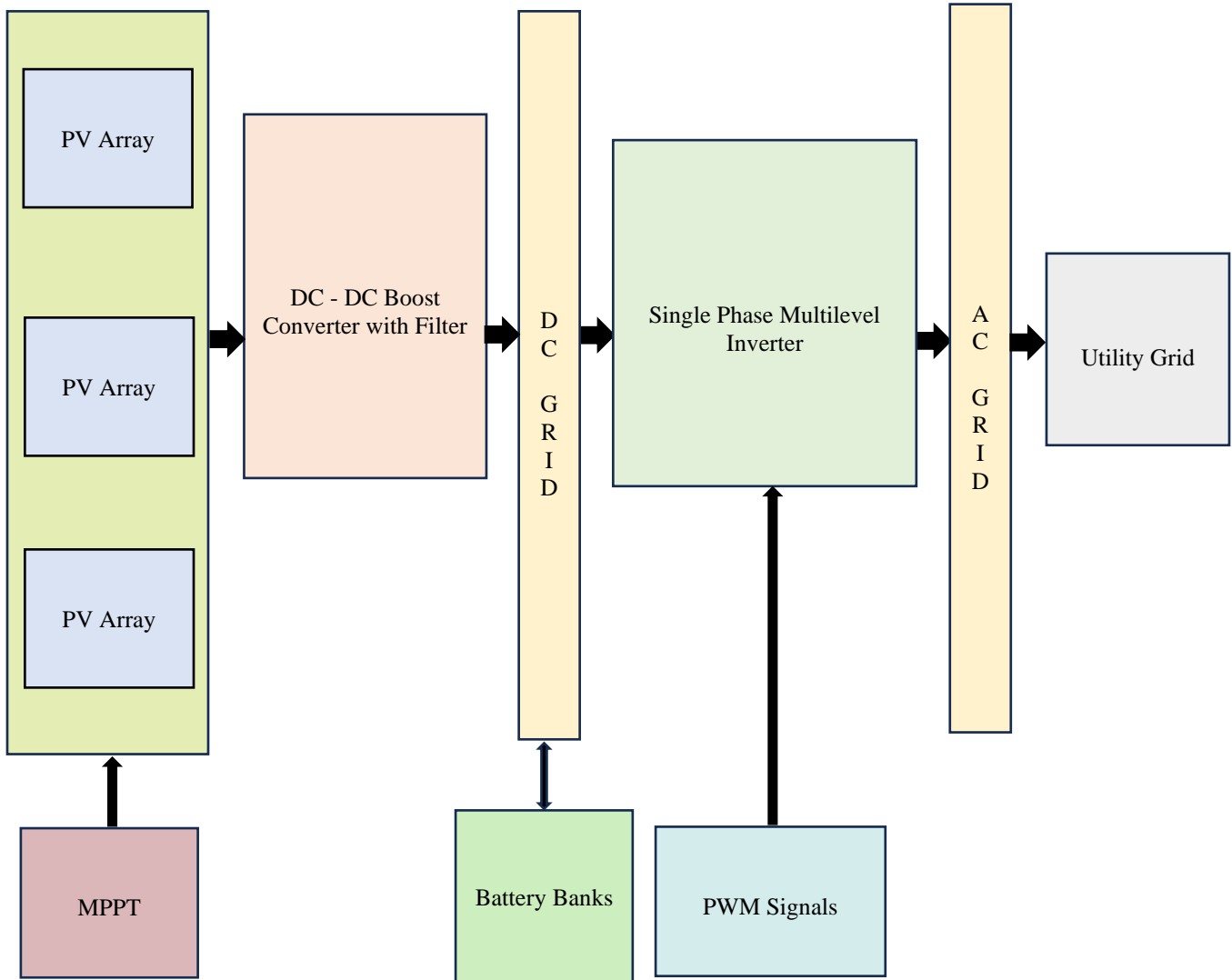


Fig. 1 PV-connected MLI with grid system

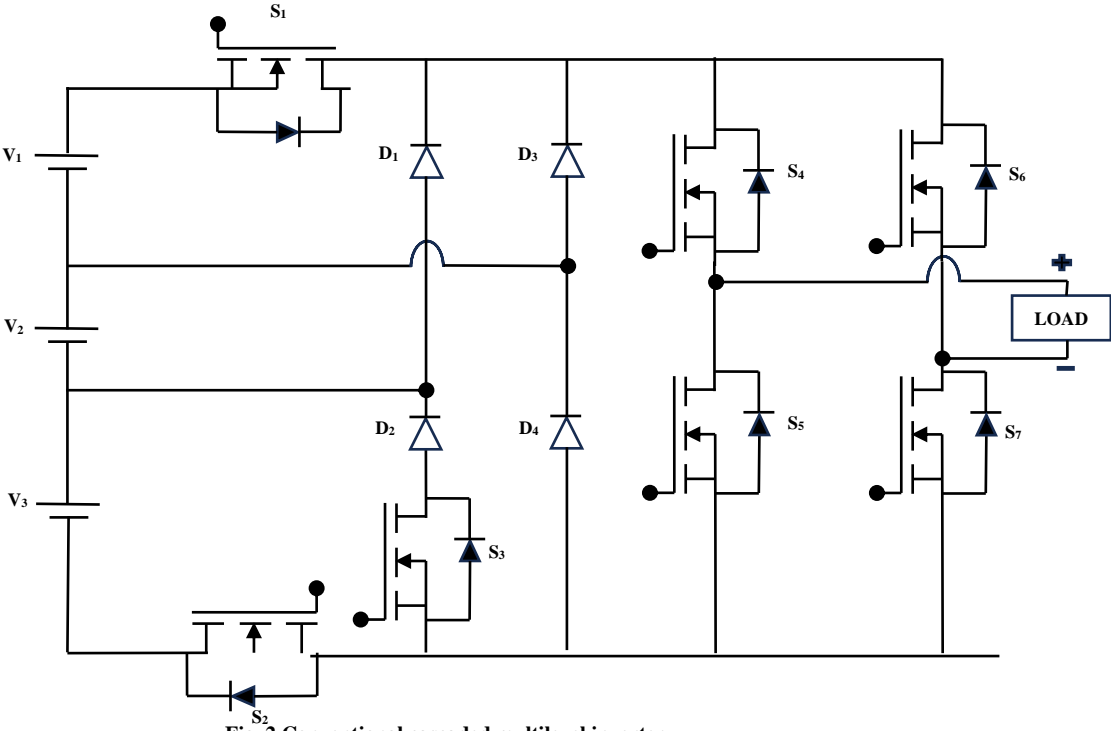


Fig. 2 Conventional cascaded multilevel inverter

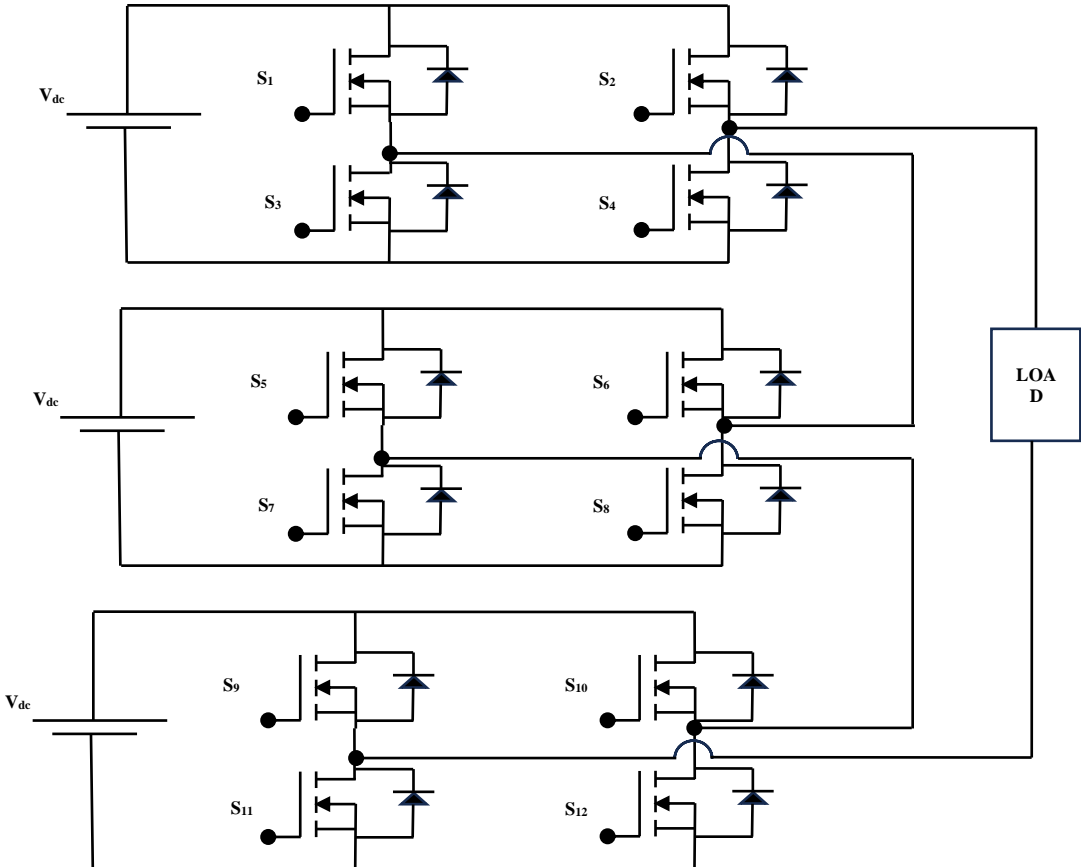


Fig. 3 Modified multilevel inverter

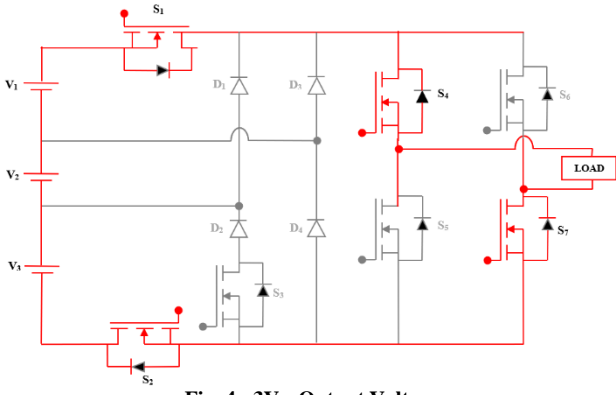


Fig. 4 +3V_{dc} Output Voltage

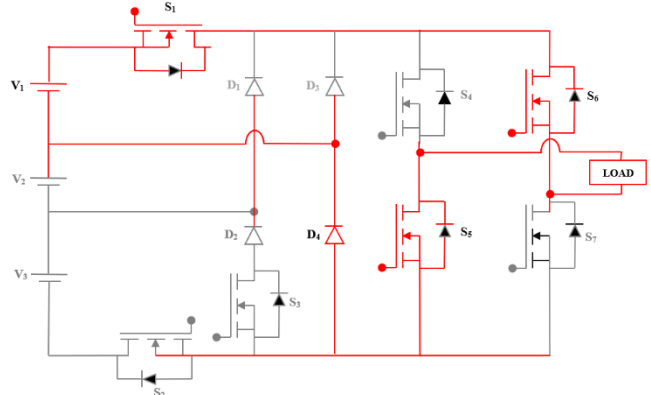


Fig. 8 -V_{dc} Output Voltage

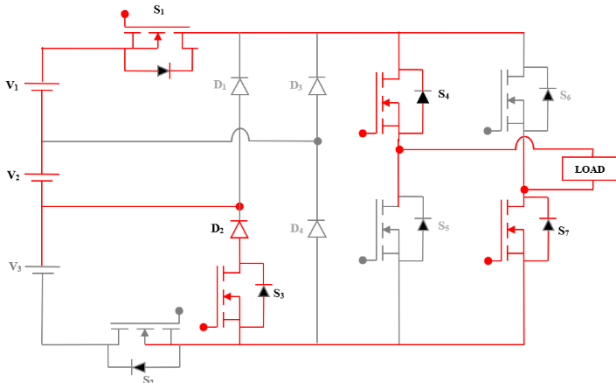


Fig. 5 +2V_{dc} Output Voltage

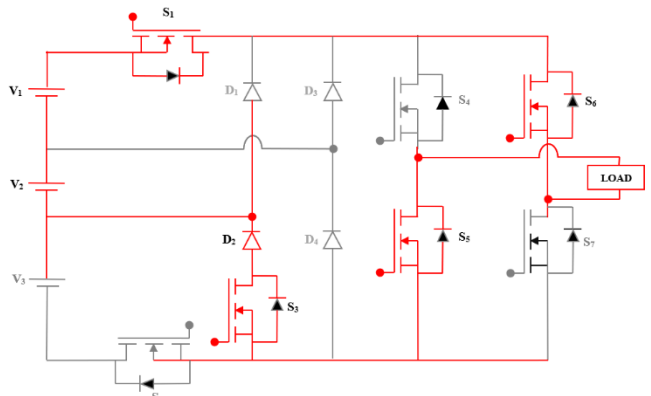


Fig. 9 -2V_{dc} Output Voltage

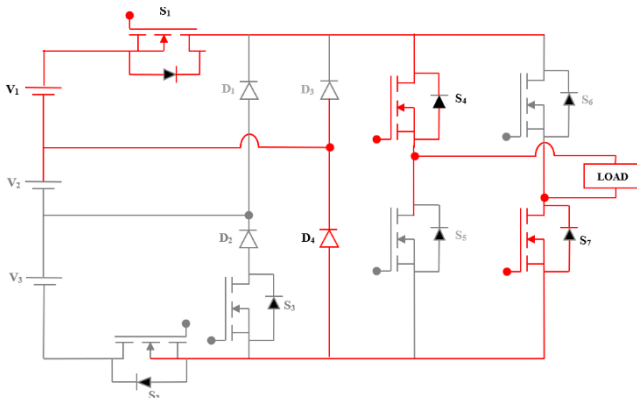


Fig. 6 +V_{dc} Output Voltage

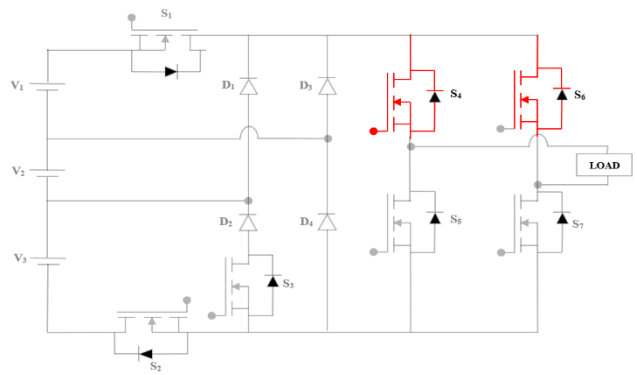


Fig. 7 +0V_{dc} Output Voltage

Figure 11 depicts the sinusoidal pulse width modulation approach used in the proposed seven-level Multilevel Inverter to control the switching pulses of power semiconductor devices.

This approach is essential for waveform shaping, ensuring the output voltage waveform closely resembles a pure sinusoidal waveform, hence reducing harmonic distortion and improving power quality.

The SPWM method used in this inverter incorporates six triangular carrier waves of the same frequency (f_c) and amplitude, aligned with the seven output voltage levels ($\pm 3V_{dc}$, $\pm 2V_{dc}$, $\pm V_{dc}$, and $0V$).

The high-frequency carrier signals are juxtaposed with a low-frequency sinusoidal reference wave (f_r), often established at the fundamental frequency of 50 Hz. When the sinusoidal reference wave surpasses a certain threshold of the carrier wave, a switching signal is activated, toggling the appropriate power switches (S_1 to S_7) ON or OFF. The inverter employs several carrier signals to produce stepped voltage levels, therefore decreasing THD and enhancing waveform smoothness. The modified MLI attains a THD of 10.5% at a modulation index of $m = 0.95$, much lower than that of traditional two-level inverters.

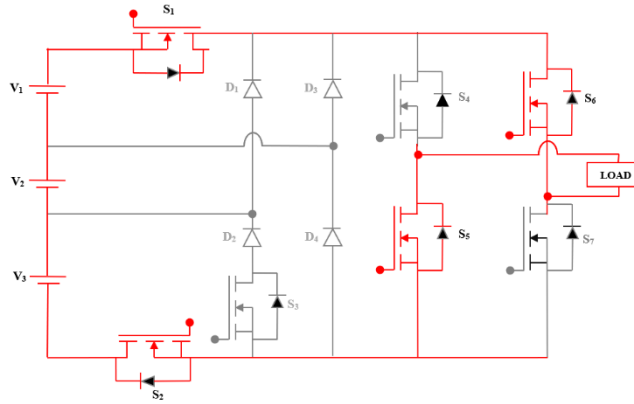


Fig. 10 -3V_{dc} Output Voltage

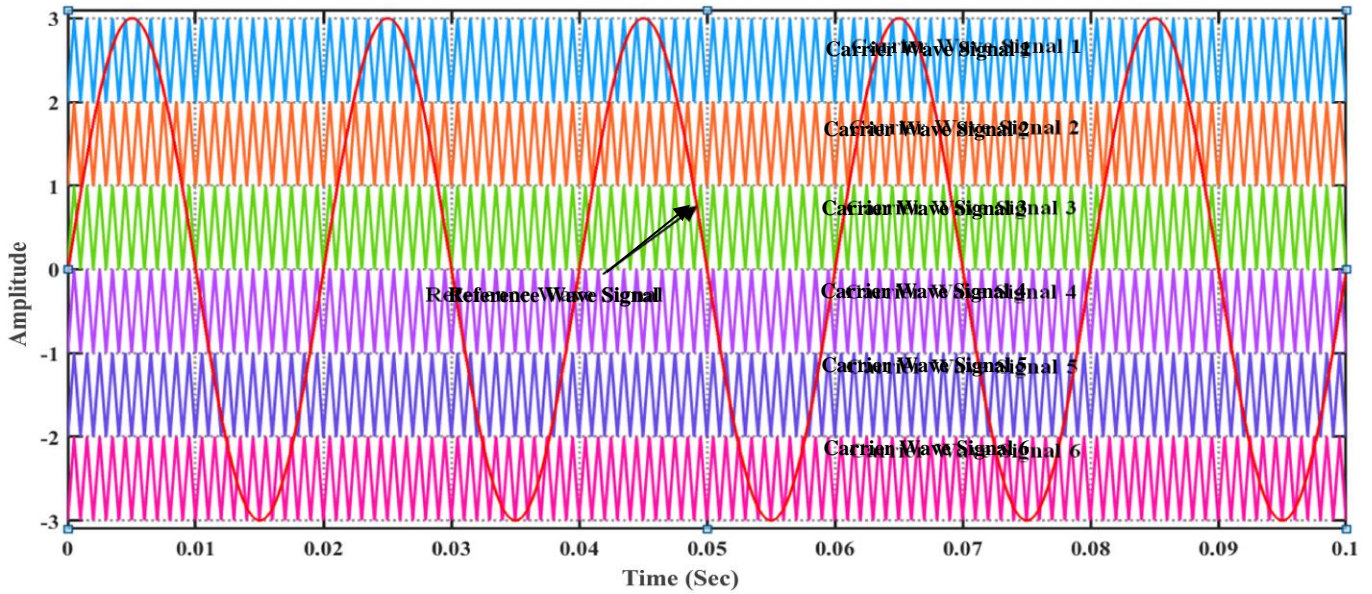


Fig. 11 Sinusoidal pulse width modulation technique for switching control

Total power loss of modified MLI can be calculated from equation (1),

$$P_{Loss} = P_{Cond} + P_{SW} \quad (1)$$

Total conduction loss of modified MLI can be calculated from equation (2),

$$P_{Cond} = \sum_{i=1}^n (V_{DS(on)} I_{rms(i)} + R_{DS(on)} I_{rms(i)}^2) \quad (2)$$

Conduction loss of individual power MOSFET from 1 to 7 can be calculated from equations (3) to (9), respectively.

$$P_{Cond1} = V_{DS(on)} I_{rms1} + R_{DS(on)} I_{rms1}^2 \quad (3)$$

$$P_{Cond2} = V_{DS(on)} I_{rms2} + R_{DS(on)} I_{rms2}^2 \quad (4)$$

$$P_{Cond3} = V_{DS(on)} I_{rms3} + R_{DS(on)} I_{rms3}^2 \quad (5)$$

$$P_{Cond4} = V_{DS(on)} I_{rms4} + R_{DS(on)} I_{rms4}^2 \quad (6)$$

$$P_{Cond5} = V_{DS(on)} I_{rms5} + R_{DS(on)} I_{rms5}^2 \quad (7)$$

$$P_{Cond6} = V_{DS(on)} I_{rms6} + R_{DS(on)} I_{rms6}^2 \quad (8)$$

$$P_{Cond7} = V_{DS(on)} I_{rms7} + R_{DS(on)} I_{rms7}^2 \quad (9)$$

The overall conduction power loss can be calculated from the expression (10),

$$P_{Cond} = P_{Cond1} + P_{Cond2} + P_{Cond3} + P_{Cond4} + P_{Cond5} + P_{Cond6} + P_{Cond7} \quad (10)$$

The overall switching loss can be calculated from expression (11), the individual switching loss can be calculated from expressions (12) to (18), and the total power switching loss can be calculated from expression (19).

$$P_{SW} = \sum_{i=1}^n \left(\frac{1}{2} V_{dc} I_{load} f_s (t_{on(i)} + t_{off(i)}) \right) \quad (11)$$

$$P_{SW1} = \frac{1}{2} V_{dc} I_{load} f_s (t_{on1} + t_{off1}) \quad (12)$$

$$P_{SW2} = \frac{1}{2} V_{dc} I_{load} f_s (t_{on2} + t_{off2}) \quad (13)$$

$$P_{SW3} = \frac{1}{2} V_{dc} I_{load} f_s (t_{on3} + t_{off3}) \quad (14)$$

$$P_{SW4} = \frac{1}{2} V_{dc} I_{load} f_s (t_{on4} + t_{off4}) \quad (15)$$

$$P_{SW5} = \frac{1}{2} V_{dc} I_{load} f_s (t_{on5} + t_{off5}) \quad (16)$$

$$P_{SW6} = \frac{1}{2} V_{dc} I_{load} f_s (t_{on6} + t_{off6}) \quad (17)$$

$$P_{SW7} = \frac{1}{2} V_{dc} I_{load} f_s (t_{on7} + t_{off7}) \quad (18)$$

$$P_{SW} = P_{SW1} + P_{SW2} + P_{SW3} + P_{SW4} + P_{SW5} + P_{SW6} + P_{SW7} \quad (19)$$

The diode power loss can be calculated from expression (20), and the Gate drive power loss can be expressed in equation (21).

$$P_{Diode} = \sum_{i=1}^n V_f I_{rms(i)} \quad (20)$$

$$P_{Gate} = \sum_{i=1}^n Q_g V_{GS} f_s \quad (21)$$

The overall efficiency, output power, input power, THD calculation, modulation index (m), and power factor (PF) can be calculated from expressions (22) to (27), respectively.

$$\eta = \frac{P_{Out}}{P_{In}} \times 100 \quad (22)$$

$$P_{Out} = V_{rms} I_{rms} \cos\phi \quad (23)$$

$$P_{In} = P_{Loss} + P_{Out} \quad (24)$$

$$THD = \frac{1}{m} \times 100\% \quad (25)$$

$$m = \frac{V_m}{V_{dc}} \quad (26)$$

$$PF = \cos(\theta) \quad (27)$$

The parameters used in the equations for calculating power loss, efficiency, and performance of the modified MLI include various electrical characteristics. The MOSFET drain-to-source voltage drop ($V_{DS(on)}$) and drain-to-source on-state resistance ($R_{DS(on)}$) determine conduction losses in the switching devices. The RMS current through each switch (I_{rms}) and output voltage (V_{rms}) influence the overall power dissipation. The number of conducting MOSFETs (n) affects both conduction and switching losses, while the DC supply link voltage (V_{dc}) serves as the primary input power source. The switching frequency (f_s) plays a crucial role in determining switching losses, as higher frequencies lead to increased power dissipation.

The gate-to-source voltage (V_{GS}) and gate charge (Q_g) define the gate drive power loss required for efficient operation. The switch turn-on and turn-off times (t_{on} and t_{off}) impact the dynamic performance and transient losses of the inverter. The diode forward voltage (V_f) is essential in evaluating diode conduction losses, while the load current (I_{load}) influences overall system efficiency, power factor, and THD. These parameters collectively determine the electrical and thermal performance of the proposed MLI, ensuring optimal operation under varying load conditions.

4. Results and Discussion

Figure 12 depicts the output voltage waveform of the proposed seven-level multilevel inverter under standard operating circumstances. The stepped waveform has seven discrete voltage levels ($\pm 3V_{dc}$, $\pm 2V_{dc}$, $\pm V_{dc}$, and $0V$), so it significantly reduces THD. The waveform is produced by an optimised switching sequence, which guarantees reduced switching losses and voltage equilibrium. The inverter attains a maximum output voltage of 308.75V at a modulation index (m) of 0.95, hence validating its high efficiency of 98%. In comparison to conventional inverters, the modified MLI offers superior waveform quality, reduced power dissipation (180W), and enhanced voltage management, making it appropriate for renewable energy systems. Figure 13 illustrates the output current waveform of the proposed seven-level MLI, which preserves sinusoidal features with less distortion. The inverter facilitates a seamless current shift, guaranteeing little ripple content. The THD of the output current is 7.37%, much lower than that of ordinary inverters. The modified topology lowers conduction losses and enhances

the power factor (0.93) under resistive-inductive load circumstances. Figure 14 illustrates the impact of inductive filtering on the output current waveform during inverter operation with an RL load. Inductive filtering efficiently smooths the current waveform, diminishes higher-order harmonic components, and improves power quality. The waveform demonstrates enhanced stability, guaranteeing that voltage and current stay in synchrony. The use of inductive filtering mitigates EMI and guarantees a power factor of 0.93. Figure 15 illustrates the THD analysis of the output voltage waveform produced by the proposed MLI. At a fundamental frequency of 50Hz, the THD is recorded at 12.27%, much lower than that of traditional two-level inverters. The stepped voltage waveform of the seven-level multilevel inverter reduces harmonic distortions, hence enhancing the voltage waveform's resemblance to a pure sine wave.

The decrease in THD enhances grid compatibility, reducing the need for external filters. Figure 16 illustrates the THD analysis of the output current waveform, indicating a THD of 7.37% at a fundamental frequency of 50Hz. The modified MLI efficiently mitigates current harmonics, guaranteeing a seamless current flow. The decrease in THD reduces power losses, electromagnetic interference, and thermal impacts in power equipment. The modified topology has a high-power factor of 0.93, enhancing grid integration and power system reliability. Figure 17 depicts the inverter's output current response to an abrupt load shift at 0.1 seconds.

The picture illustrates that the modified MLI rapidly adjusts to load fluctuations, maintaining steady current management without significant oscillations. The inverter ensures seamless current shifts, minimising transient disturbances. Figure 18 illustrates the inverter's reaction as the load transitions from purely Resistive (R) to Resistive-Inductive (RL) at 0.1 seconds. The illustration depicts a consistent current waveform transition, guaranteeing little distortion and power variation. Under resistive-inductive load circumstances, the power factor is sustained at 0.93, and efficiency exceeds 91%, demonstrating the inverter's tolerance

to load fluctuations. Figure 19 juxtaposes the performance metrics of traditional multilevel inverters (CHB, FC, and NPC) with the proposed seven-level multilevel inverter. The modified topology necessitates just 7 switches, 3 DC sources, and 4 diodes, in contrast to traditional CHB, FC, and NPC MLIs, which use 12 switches, several capacitors, or supplementary clamping diodes. The modified inverter has an efficiency of 98%, surpassing CHB (96%), FC (95%), and NPC (96%). The modified topology exhibits the lowest total harmonic distortion, hence assuring superior power quality. Figure 20 depicts the influence of modulation index (m) on output voltage, THD, power loss, and efficiency. At $m = 0.95$, the inverter attains an output voltage of 308.75V, a THD of 10.5%, a power loss of 180W, and an efficiency of 92.2%. As m grows, efficiency improves and THD diminishes, illustrating the efficacy of SPWM in harmonics reduction. Table 1 contrasts CHB, FC, NPC, and the proposed seven-level MLI in terms of component count, efficiency, and complexity. The modified topology necessitates just 7 switches and 4 diodes, in contrast to CHB (12 switches), FC (6 capacitors), and NPC (6 diodes). The modified MLI attains 98% efficiency, surpassing CHB (96%), FC (95%), and NPC (96%). It has minimal control complexity, straightforward voltage balancing, and high fault tolerance, making it a cost-effective and efficient option for photovoltaic-grid applications. Table 2 analyses the influence of modulation index (m) on output voltage, THD, power loss, and efficiency. At $m = 0.95$, the inverter produces an output of 308.75V, exhibits a total harmonic distortion of 10.5%, incurs a power loss of 180W, and achieves an efficiency of 92.2%. Enhancing m augments efficiency and diminishes THD, hence assuring superior power quality. The minimisation of switching and conduction losses enhances the power factor (0.95) and overall grid performance. Table 3 juxtaposes R and RL loads, illustrating changes in efficiency. Resistive loads attain an efficiency of up to 94.6%, but RL loads see a little reduction in efficiency to 91.3% owing to reactive components. The power factor decreases from 1 (pure resistive load) to 0.79 (high resistive-inductive load). The inverter maintains consistent efficiency under variable load circumstances, demonstrating its appropriateness for practical applications.

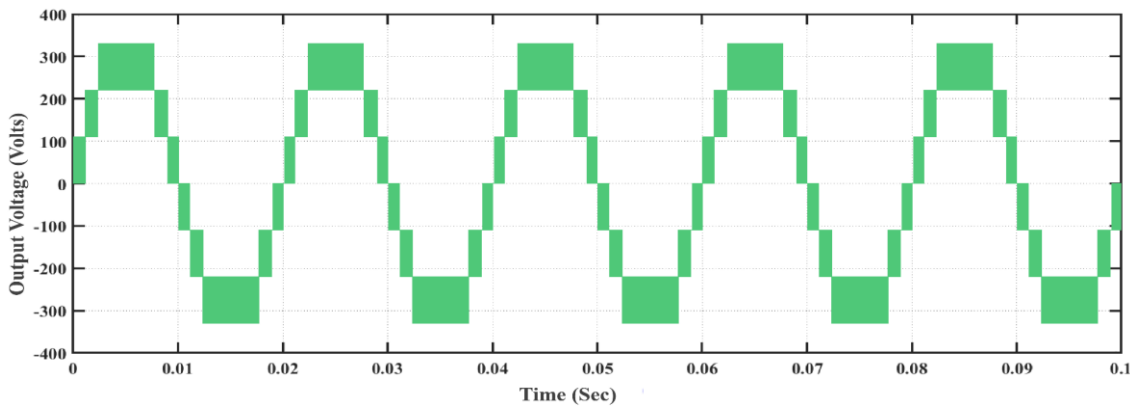


Fig. 12 Output Voltage Waveform of the Proposed Seven-Level Multilevel Inverter

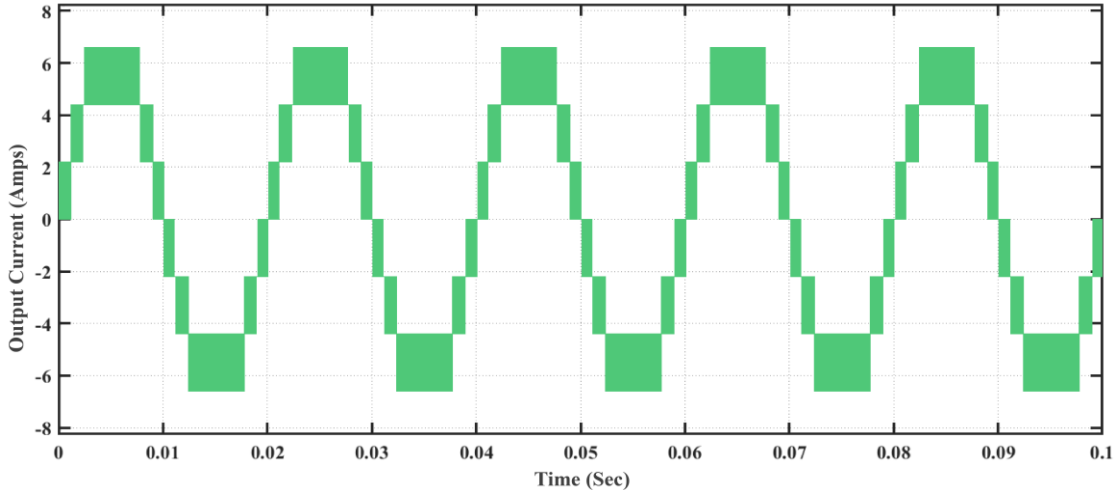


Fig. 13 Output Current Waveform of the Proposed Seven-Level Multilevel Inverter

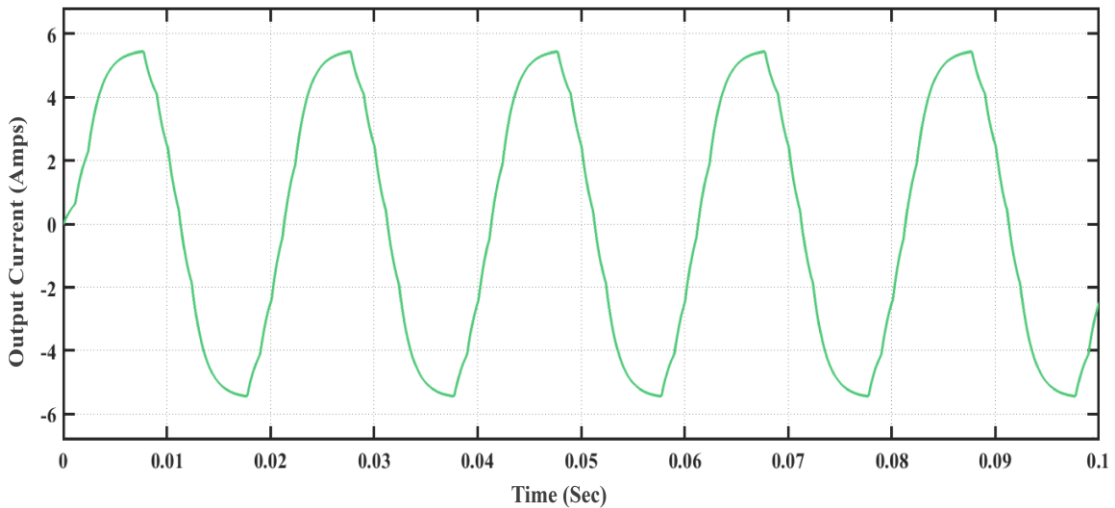


Fig. 14 Filtered Output Current Response Under Inductive Load Conditions

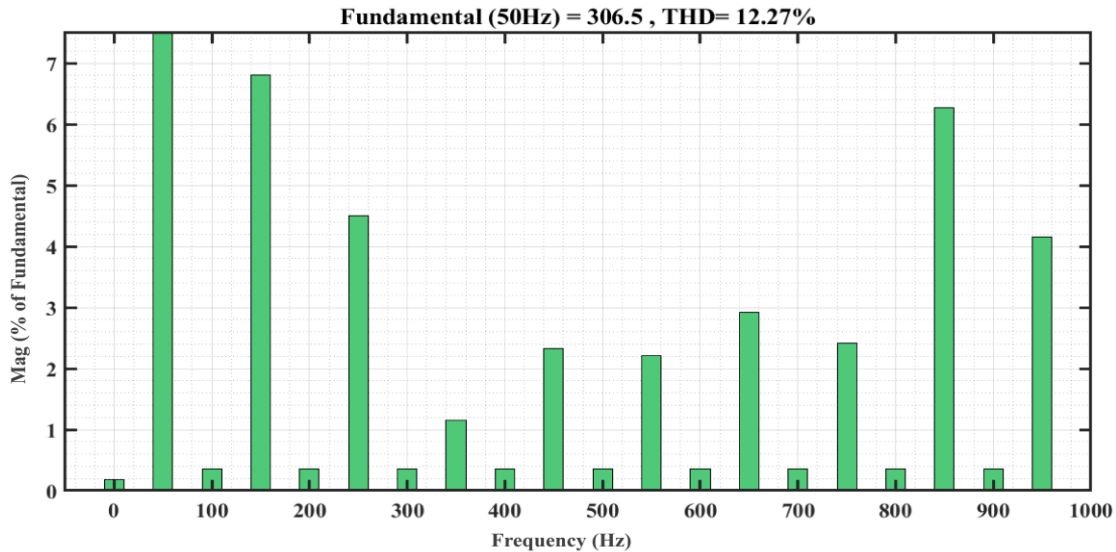


Fig. 15 Total Harmonic Distortion (THD) Analysis of Output Voltage

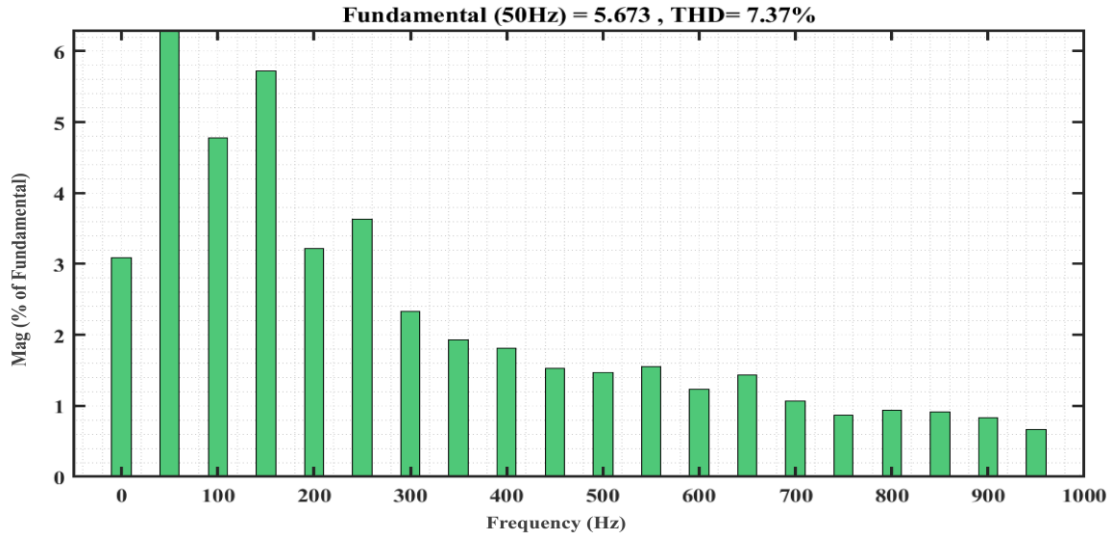


Fig. 16 Total Harmonic Distortion (THD) Analysis of Output Current

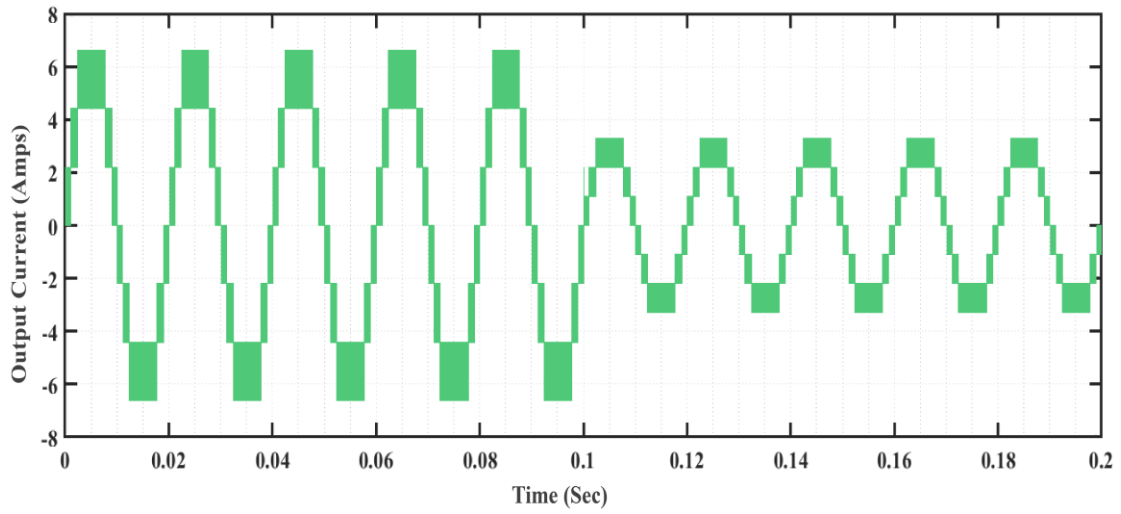


Fig. 17 Dynamic Response of Load Current Change After 0.1 Seconds

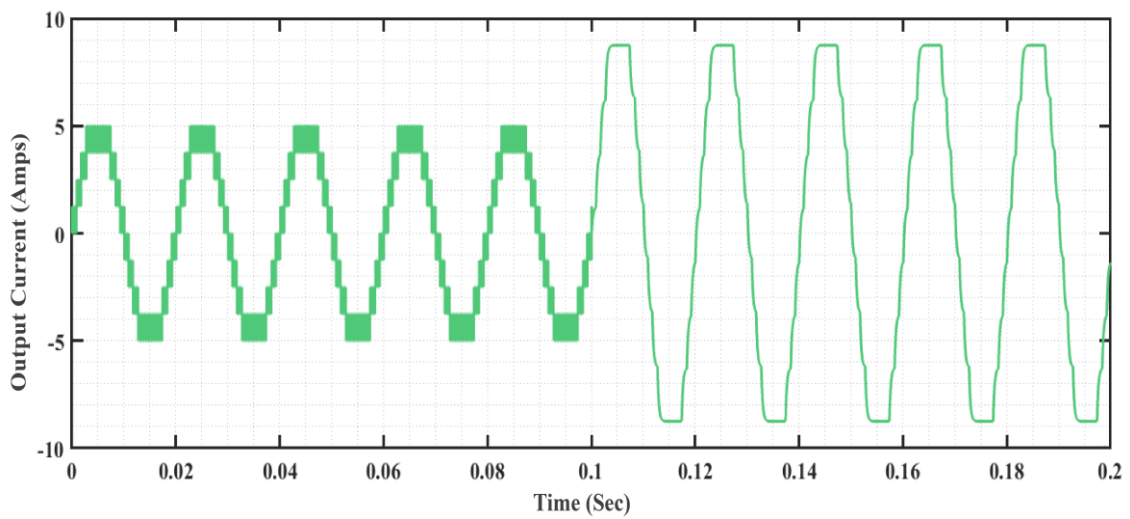


Fig. 18 Transition from Resistive (R) to Resistive-Inductive (RL) Load at 0.1 Seconds

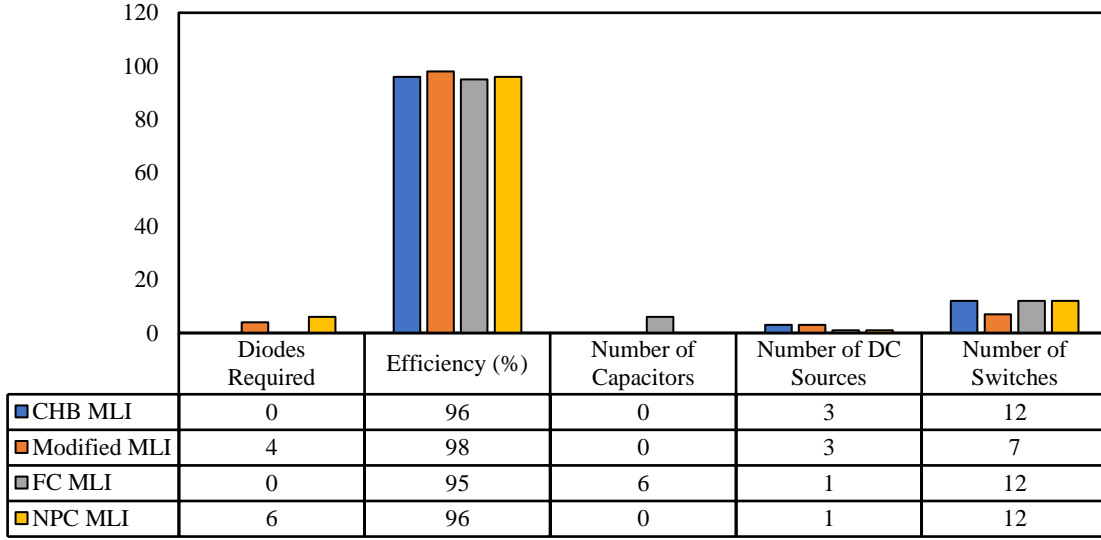


Fig. 19 Performance comparison of conventional and proposed multilevel inverters

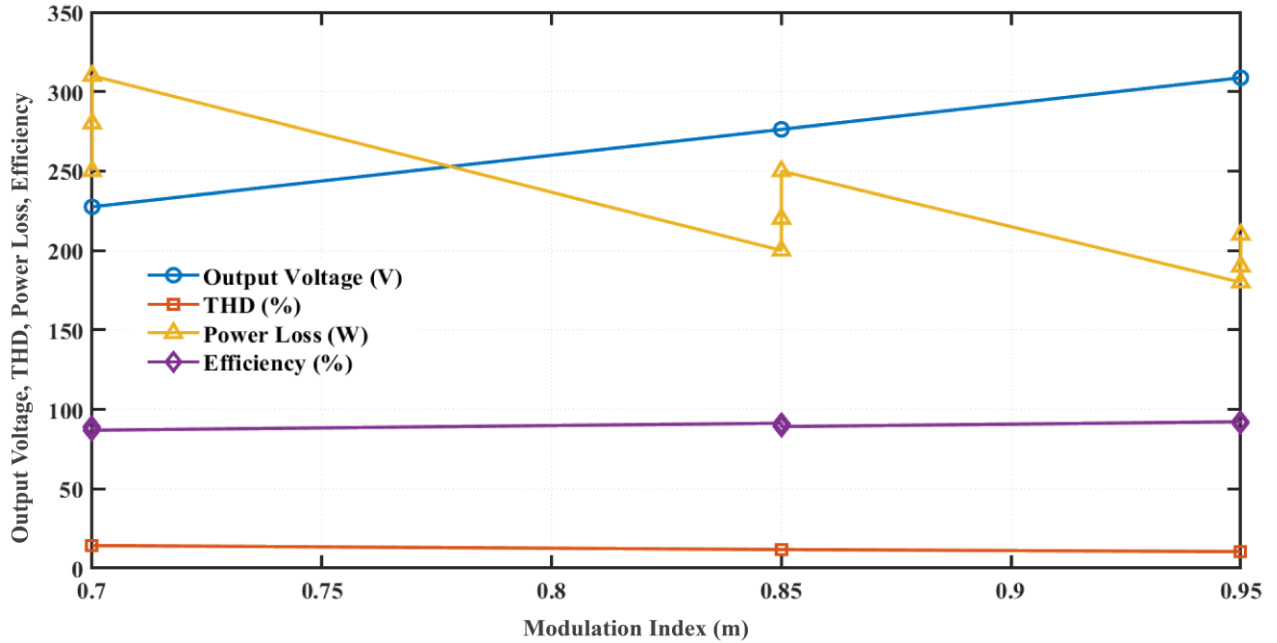


Fig. 20 Effect of Modulation Index on Output Voltage, THD, Power Loss, and Efficiency

Table 1. Comparison of conventional and modified Seven-Level MLI

Parameters	CHB - MLI	FC - MLI	NPC - MLI	Modified - MLI
Number of DC Sources	3	1	1	3
Number of Capacitors	0	6	0	0
Number of Switches	12	12	12	7
Diodes Required	0	0	6	4
Voltage Balancing	Simple	Complex	Medium	Simple
Control Complexity	Moderate	High	High	Low
Fault Tolerance	Low	High	Medium	High
THD (Total Harmonic Distortion)	Low	Lowest	Low	Lowest
Efficiency (%)	96	95	96	98
Cost (Relative)	Medium	High	Medium	Low

Table 2. Impact of modulation index on output voltage, THD, and power loss

Modulation Index (m)	Output Voltage (V)	THD (%)	Power Loss (W)	Efficiency (%)	Switching Loss (W)	Cond. Loss (W)	PF	Load Resistance (R)	Load Impedance (Z)
0.70	227.50	12.5	310	90.2	155	155	0.75	35	40
0.70	227.50	12.5	280	91.3	140	140	0.80	35	40
0.70	227.50	12.5	250	91.6	120	130	0.85	35	40
0.85	276.25	10.7	230	92.2	115	115	0.85	35	40
0.85	276.25	10.7	220	92.7	110	110	0.87	35	40
0.85	276.25	10.7	210	93.3	105	105	0.90	35	40
0.95	308.75	7.3	200	94.5	95	105	0.92	35	40
0.95	308.75	7.3	190	95.8	90	100	0.93	35	40
0.95	308.75	7.3	180	96.1	85	95	0.95	35	40

Table 3. Impact of Load Changes on Efficiency and Power Factor

Load Type	R (Ω)	X _L (Ω)	Z (Ω)	THD (%)	Power Loss (W)	Efficiency (%)	PF	Switching Loss (W)	Conduction Loss (W)
R Load	50	0	50.00	15.0	120	94.60	1	60	60
	40	0	40.00	16.0	150	93.30	1	75	75
	30	0	30.00	17.5	180	91.50	1	90	90
RL Load	50	20	53.85	16.2	135	93.00	0.93	70	65
	50	30	58.30	17.0	145	92.30	0.86	75	70
	50	40	63.20	18.5	160	91.30	0.79	85	75
	40	20	44.72	15.8	140	92.80	0.95	65	75
	40	30	50.00	16.8	155	91.70	0.87	75	80
	40	40	56.60	18.0	175	90.40	0.8	90	85
	30	20	36.05	16.0	150	92.30	0.96	70	80
	30	30	40.00	17.2	165	91.20	0.89	80	85

5. Conclusion

The outlined seven-level MLI offers an efficient and economical solution for renewable energy applications, especially in PV grid integration. The modified inverter employs three DC sources, four diodes, and seven switches to minimise switching losses, conduction losses, and THD, attaining an efficiency of 98%. The optimised switching approach guarantees a segmented output voltage waveform, enhancing power quality and diminishing electromagnetic interference (EMI). In comparison to traditional CHB, FC, and NPC MLIs, the modified topology exhibits substantial improvements in efficiency, voltage equilibrium, and fault tolerance, making it an optimal choice for medium- and high-power applications. The SPWM approach, using multiple carrier waves, successfully decreases THD to 10.5% at a

modulation index of 0.95, hence producing a smooth sinusoidal waveform that improves grid stability. The inverter sustains a steady power factor of 0.93 under resistive-inductive load circumstances, demonstrating its reliable performance across diverse load situations. Simulation results validate that the proposed MLI offers superior voltage control, reduced component stress, and enhanced reliability relative to conventional topologies. The dynamic load response research indicates that the inverter rapidly adjusts to load fluctuations, guaranteeing a continuous power supply. Future study may concentrate on enhancing modulation tactics, refining fault diagnostic systems, and using AI-driven MPPT approaches to achieve superior renewable energy conversion efficiency. The modified seven-level MLI is a viable option for next-generation power electronics, fostering a sustainable and energy-efficient future.

References

- [1] Marcos García-López, Borja Montano, and Joaquín Melgarejo, "Household Energy Consumption and the Financial Feasibility of Self-Consumption through Photovoltaic Panels in Spain," *Energy Efficiency*, vol. 16, no. 6, pp. 1-17, 2023. [CrossRef] [Google Scholar] [Publisher Link]
- [2] Ahmed M.T. Ibraheem Al-Naib, and Majeed Ismail Mohammed, "IoT-Based Real Time Data Acquisition of PV Panel," *IEEE International Conference on Engineering, Science and Advanced Technology*, Mosul, Iraq, pp. 169-173, 2023. [CrossRef] [Google Scholar] [Publisher Link]
- [3] Asier del Rio et al., "Particle Swarm Optimization-Based Control for Maximum Power Point Tracking Implemented in a Real Time Photovoltaic System," *Information*, vol. 14, no. 10, pp. 1-16, 2023. [CrossRef] [Google Scholar] [Publisher Link]

- [4] Kemal Bilen, and İsmail Erdoğan, “Effects of Cooling on Performance of Photovoltaic/Thermal (PV/T) Solar Panels: A Comprehensive Review,” *Solar Energy*, vol. 262, 2023. [[CrossRef](#)] [[Google Scholar](#)] [[Publisher Link](#)]
- [5] Ahmed Hussain Elmetwaly et al., “Modeling, Simulation, and Experimental Validation of a Novel MPPT for Hybrid Renewable Sources Integrated with UPQC: An Application of Jellyfish Search Optimizer,” *Sustainability*, vol. 15, no. 6, pp. 1-30, 2023. [[CrossRef](#)] [[Google Scholar](#)] [[Publisher Link](#)]
- [6] Mohammed Chaker et al., “Development of a PV Emulator using SMPS Converter and a Model Selection Mechanism for Characteristic Generation,” *Solar Energy*, vol. 239, pp. 117-128, 2022. [[CrossRef](#)] [[Google Scholar](#)] [[Publisher Link](#)]
- [7] Abdelkadir Boucharef et al., “Solar Module Emulator Based on a Low-Cost Microcontroller,” *Measurement*, vol. 187, 2022. [[CrossRef](#)] [[Google Scholar](#)] [[Publisher Link](#)]
- [8] A. Nazar Ali et al., “Design and Development of Realistic PV Emulator Adaptable to the Maximum Power Point Tracking Algorithm and Battery Charging Controller,” *Solar Energy*, vol. 220, pp. 473-490, 2021. [[CrossRef](#)] [[Google Scholar](#)] [[Publisher Link](#)]
- [9] Javed Ahmad et al., “Performance Analysis and Hardware-in-the-Loop (HIL) Validation of Single Switch High Voltage Gain DC-DC Converters for MPP Tracking in Solar PV System,” *IEEE Access*, vol. 9, pp. 48811-48830, 2021. [[CrossRef](#)] [[Google Scholar](#)] [[Publisher Link](#)]
- [10] Nabil A. Ahmed, Salahuddin Abdul Rahman, and Bader N. Alajmi, “Optimal Controller Tuning for P&O Maximum Power Point Tracking of PV Systems Using Genetic and Cuckoo Search Algorithms,” *International Transactions on Electrical Energy Systems*, vol. 31, no. 10, 2020. [[CrossRef](#)] [[Google Scholar](#)] [[Publisher Link](#)]
- [11] Cagfer Yanarates, Yidong Wang, and Zhongfu Zhou, “Unity Proportional Gain Resonant and Gain Scheduled Proportional (PR-P) Controller-Based Variable Perturbation Size Real-Time Adaptive Perturb and Observe (PO) MPPT Algorithm for PV Systems,” *IEEE Access*, vol. 9, pp. 138468-138482, 2021. [[CrossRef](#)] [[Google Scholar](#)] [[Publisher Link](#)]
- [12] Habes Ali Khawaldeh et al., “Efficiency Improvement Scheme for PV Emulator Based on a Physical Equivalent PV-Cell Model,” *IEEE Access*, vol. 9, pp. 83929-83939, 2021. [[CrossRef](#)] [[Google Scholar](#)] [[Publisher Link](#)]
- [13] Chao-Tsung Ma et al., “Design and Implementation of a Flexible Photovoltaic Emulator Using a Gan-Based Synchronous Buck Converter,” *Micromachines*, vol. 12, no. 12, pp. 1-16, 2021. [[CrossRef](#)] [[Google Scholar](#)] [[Publisher Link](#)]
- [14] Habes A. Khawaldeh et al., “Fast Photovoltaic Emulator Based on PV-Cell Equivalent Circuit Model,” *IEEE 12th Energy Conversion Congress and Exposition - Asia*, Singapore, pp. 2121-2126, 2021. [[CrossRef](#)] [[Google Scholar](#)] [[Publisher Link](#)]
- [15] Dan Craciunescu, and Laurentiu Fara, “Investigation of the Partial Shading Effect of Photovoltaic Panels and Optimization of Their Performance Based on High-Efficiency FLC Algorithm,” *Energies*, vol. 16, no. 3, pp. 1-28, 2023. [[CrossRef](#)] [[Google Scholar](#)] [[Publisher Link](#)]
- [16] S. Senthilkumar et al., “Analysis of Single-Diode PV Model and Optimized MPPT Model for Different Environmental Conditions,” *International Transactions on Electrical Energy Systems*, vol. 2022, no. 1, pp. 1-17, 2022. [[CrossRef](#)] [[Google Scholar](#)] [[Publisher Link](#)]
- [17] Ambe Harrison, and Njimboh Henry Alombah, “A New Piecewise Segmentation Based Solar Photovoltaic Emulator Using Artificial Neural Networks and a Nonlinear Backstepping Controller,” *Applied Solar Energy*, vol. 59, no. 3, pp. 283-304, 2023. [[CrossRef](#)] [[Google Scholar](#)] [[Publisher Link](#)]
- [18] Venkata Dinavahi, and Ning Lin, *Adaptive Time-Stepping Based Real-Time EMT Emulation*, Real-Time Electromagnetic Transient Simulation of AC-DC Network, Wiley-IEEE Press, pp. 217-252, 2021. [[CrossRef](#)] [[Google Scholar](#)] [[Publisher Link](#)]
- [19] Karima El Hammoumi, Redouane Chaibi, and Rachid El Bachtiri, “Fuzzy State-Feedback Control for MPPT of Photovoltaic Energy with Storage System,” *International Journal of Innovative Computing, Information and Control*, vol. 18, no. 1, pp. 253-270, 2022. [[CrossRef](#)] [[Google Scholar](#)] [[Publisher Link](#)]
- [20] Mohammed Rasheed et al., “Mathematical Models for Resolving the Nonlinear Formula for Solar Cell,” *Indonesian Journal of Electrical Engineering and Computer Science*, vol. 33, no. 1, pp. 653-660, 1 2024. [[CrossRef](#)] [[Publisher Link](#)]
- [21] Benjamin Dean et al., “A Graphical User Interface Platform to Support Power Electronic Converters and Integrated Systems,” *IEEE Power and Energy Society Innovative Smart Grid Technologies Conference*, Washington, DC, USA, pp. 1-5, 2024. [[CrossRef](#)] [[Google Scholar](#)] [[Publisher Link](#)]
- [22] Razman Ayop et al., “Photovoltaic Emulator Using Error Adjustment Fuzzy Logic Proportional-Integral Controller,” *International Journal of Power Electronics and Drive Systems*, vol. 13, no. 2, pp. 1111-1118, 2022. [[CrossRef](#)] [[Google Scholar](#)] [[Publisher Link](#)]
- [23] Wenqiang Zhu et al., “A Novel Simplified Buck Power System Control Algorithm: Application to the Emulation of Photovoltaic Solar Panels,” *Computers and Electrical Engineering*, vol. 116, 2024. [[CrossRef](#)] [[Google Scholar](#)] [[Publisher Link](#)]
- [24] Saibal Manna et al., “Design and Implementation of a New Adaptive MPPT Controller for Solar PV Systems,” *Energy Reports*, vol. 9, pp. 1818-1829, 2023. [[CrossRef](#)] [[Google Scholar](#)] [[Publisher Link](#)]
- [25] Zouhaira Ben Mahmoud, Intissar Moussa, and Adel Khedher, “Implementation of MPPT Algorithms to a Developed Photovoltaic Emulator: Study and Comparative Analysis,” *In IEEE 11th International Conference on Systems and Control*, Sousse, Tunisia, pp. 719-724, 2023. [[CrossRef](#)] [[Google Scholar](#)] [[Publisher Link](#)]

- [26] Bidjagare Akiza, Edjadessamam Akoro, and Dam-Bé L. Douti, "Design and Simulation of an MPPT Charge Controller for a PV Application," In *2nd German-West African Conference on Sustainable, Renewable Energy Systems, TH Wildau Engineering and Natural Sciences Proceedings*, vol. 1, pp. 257-261, 2021. [[CrossRef](#)] [[Google Scholar](#)] [[Publisher Link](#)]
- [27] Abdulwahab A. Q. Hasan, Ammar Ahmed Alkahtani, and Nowshad Amin, "Modeling and Performance Evaluation of Solar Cells Using I-V Curve Analysis," *Proceedings of the 2nd International Conference on Emerging Technologies and Intelligent Systems*, pp. 643-650, 2023. [[CrossRef](#)] [[Google Scholar](#)] [[Publisher Link](#)]
- [28] Haonan Fang et al., "A Linearization Based Model Equivalent Method for Distributed Photovoltaic Generation Clusters," In *IEEE 6th Conference on Energy Internet and Energy System Integration (EI2)*, Chengdu, China, pp. 1-5, 2022. [[CrossRef](#)] [[Google Scholar](#)] [[Publisher Link](#)]
- [29] Ahmed Shawki Jaber et al., "Comparasion the Electrical Parameters of Photovoltaic Cell Using Numerical Methods," *EUREKA: Physics and Engineering*, vol. 4, no. 4, pp. 29-39, 2023. [[CrossRef](#)] [[Google Scholar](#)] [[Publisher Link](#)]
- [30] Lsmail Hburi, Hasan Fahad, and Ali Assad. "Powerful Maximum Power Point Tracking for PV Systems: An Artificial Intelligence Paradigm," *IEEE Iraqi International Conference on Communication and Information Technologies*, Basrah, Iraq, pp. 280-286, 2022. [[CrossRef](#)] [[Google Scholar](#)] [[Publisher Link](#)]
- [31] Suleyman Adak et al., "Thevenin Equivalent of Solar PV Cell Model and Maximum Power Transfer," *IEEE International Conference on Electrical, Communication, and Computer Engineering*, Kuala Lumpur, Malaysia, pp. 1-5, 2021. [[CrossRef](#)] [[Google Scholar](#)] [[Publisher Link](#)]
- [32] Victor Daldegan Paduani et al., "A Unified Power-Setpoint Tracking Algorithm for Utility-Scale PV Systems with Power Reserves and Fast Frequency Response Capabilities," *IEEE Transactions on Sustainable Energy*, vol. 13, no. 1, pp. 479-490, 2022. [[CrossRef](#)] [[Google Scholar](#)] [[Publisher Link](#)]
- [33] Mahendiran Vellingiri et al., "Non-Linear Analysis of Novel Equivalent Circuits of Single-Diode Solar Cell Models with Voltage-Dependent Resistance," *Fractal and Fractional*, vol. 7, no. 1, pp. 1-26, 2023. [[CrossRef](#)] [[Google Scholar](#)] [[Publisher Link](#)]
- [34] Maria Amaidi, Lassaad Zaaoui, and Ali Mansouri, "Enhanced Method for Estimating Unknown Parameters in Single Diode Model for Solar Photovoltaic Cells," *Malaysian Journal of Fundamental and Applied Sciences*, vol. 20, no. 3, pp. 648-660, 2024. [[CrossRef](#)] [[Google Scholar](#)] [[Publisher Link](#)]
- [35] Imade Choulli et al., "A Novel Hybrid Analytical/Iterative Method to Extract the Single-Diode Model's Parameters Using Lambert's W-Function," *Energy Conversion and Management: X*, vol. 18, 2023. [[CrossRef](#)] [[Google Scholar](#)] [[Publisher Link](#)]